Surface-induced stacking transition at SiC(0001)

M. C. Righi, C. A. Pignedoli, G. Borghi, R. Di Felice, and C. M. Bertoni
INFM-National Research Center on nanoStructures and bioSystems at Surfaces (S^3), Dipartimento di Fisica, Università di Modena e Reggio Emilia, Via Campi 213/A, 41100 Modena, Italy

A. Catellani
CNR-IMEM, Parco Area delle Scienze 37a, 43010 Parma, Italy

(Received 15 January 2002; published 25 July 2002)

We present the *ab initio* results for the energetics of several SiC surfaces having different underlying bulk polytypes, to investigate the role of surface effects in the mechanisms of stacking inversion in SiC. We considered the Si adatom $\sqrt{3}\times\sqrt{3}$ reconstruction for the cubic SiC(111) and the hexagonal SiC(0001) surfaces, taking into account the different subsurface bulk terminations compatible with the $4H$ and $6H$ polytypes, and allowing for two opposite stacking orientations of the topmost surface layer. Our investigation reveals that the energy differences among SiC polytypes are enhanced at the surface with respect to the bulk, and two-dimensional effects favor the formation of cubic SiC. We discuss the relevant role played by the surface energetics in the homoepitaxial growth of SiC.

DOI: 10.1103/PhysRevB.66.045320 PACS number(s): 68.35.Md, 71.15.Mb, 61.72.Nn

I. INTRODUCTION

Silicon carbide (SiC) is a unique compound semiconductor, with appealing properties for high power electronics and biological sensors. The material appears in a number of tetrahedral polytypes[1,2] whose existence rises fascinating fundamental problems and opens the way to many feasible technological applications.[3] The energy surface which determines the relative stability of these bulk phases has several almost degenerate local minima: the largest difference of only few meV occurs between the wurtzite lattice $2H$ (AB stacking sequence) and the zinc blende lattice $3C$ (ABC stacking sequence). See Fig. 1 for a schematic representation of the main silicon carbide polytypes. The existence of this variety of metastable bulk phases in a restricted energy range may be responsible for the wide stacking fault networks revealed in SiC crystals: in fact, due to the small energy difference between the polytypes, it is very easy to form different regimes during a single deposition process to fabricate the material. However, if the polytype energetics is modified at the surface layers, one may argue that a surface-controlled growth procedure may affect the stacking sequence of the grown material, favoring one polytype among all the others when performing homoepitaxy of SiC. Indeed, it was recently proposed that the surface reconstruction in hexagonal SiC might influence the stacking of newly attached bilayers. Quantitative low energy electron diffraction (LEED) experiments indicate that the cubic phase of SiC is grown by molecular beam epitaxy (MBE) on top of a Si-terminated $\sqrt{3}\times\sqrt{3}$-SiC(0001) surface, despite the hexagonal topology of the $4H$ underlying substrate.[4]

With the aim of investigating how the presence of a surface may affect the polytype stability, we performed first-principle total energy calculations for the (0001) surface of a set of possible SiC polytypes, each terminating with either a $3C$-like or a $2H$-like stacking sequence of the two outermost SiC bilayers (a bilayer consists of a Si-C bonded pair, with the bond not oriented along the [0001] axis: see Fig. 1 for the geometry). The energy required for the surface stacking inversion is evaluated through a comparative analysis of the optimized structures. According to a layer-by-layer deposition model, the grown material should exhibit a stable growth front at each deposited layer, identified by a low-energy surface. Therefore, among a set of metastable surface configurations, that with the lowest formation energy will determine the structure of the film. Our results reveal that the presence of the surface significantly affects the polytype stability: whereas the $3C$ lattice is not the lowest-energy bulk phase, we have found a clear preference of the surface for a regular continuation of the underlying stacking orientation, independently of the substrate polytype. This mechanism, which requires that a two-dimensional (2D) deposition process is achieved, favors the formation of cubic crystals. Moreover, the energy difference between the two possible opposite stacking orientations of the outermost surface bilayer at the SiC(0001) surface is larger by one order of magnitude than the energy differences characteristic of the bulk polytypes. Therefore, thermodynamic effects based on phase stability are sufficient for the selection of a given polytype. The geometrical details of the surface reconstruction, as well as the surface bandstructure, are not influenced by the surface stacking, in agreement with the observation that the tetrahedral polytypes differ only to third-nearest neighbors.

II. METHOD

We performed first-principle calculations in the scheme of the density functional theory (DFT)[5] for $3C$-, $6H$-, $4H$-, and $2H$-SiC bulk polytypes, as well as for $3C$-SiC(111) and pH-SiC(0001) surfaces ($p=4,6$) with a Si adatom $\sqrt{3}\times\sqrt{3}$ reconstruction.[6]

By performing test calculations on the structure and stability of the SiC bulk polytypes, we evaluated the accuracy of different exchange-correlation (xc) functionals: we considered the local density approximation (LDA), and two different gradient-corrected (GGA) functionals, i.e., the BLYP

 ©2002 The American Physical Society

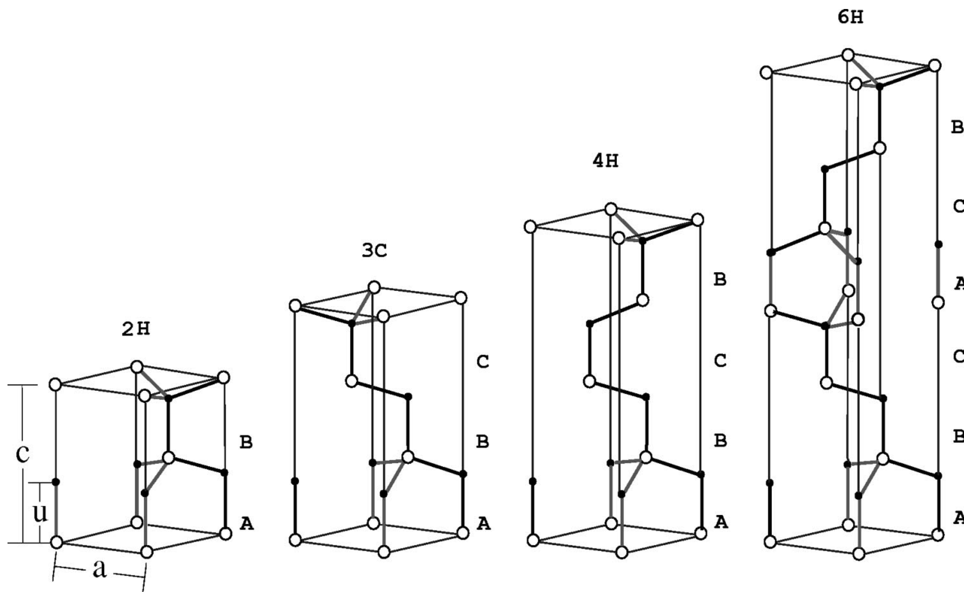

FIG. 1. Hexagonal unit cells of the $2H$, $3C$, $4H$, and $6H$ polytypes of SiC. The stacking sequence AB ($2H$), ABC ($3C$), $ABCB$ ($4H$), $ABCACB$ ($6H$), and the lattice parameters a, c, u, are indicated.

parametrization[7] and the PW91 parametrization.[8] For the surface calculations, we used the PW91 functional, motivated by its good performance in describing the bulk properties.

The ionic species were described by norm-conserving pseudopotentials,[9] which were generated employing the same xc functional adopted in the self-consistent total energy calculations. The electronic wave functions were expanded in a plane-wave basis, with a kinetic energy cutoff of 50 Ry. The completeness of the basis for an accurate description of both bulk energetics[10] and surface reconstructions[11] was checked, increasing the cutoff up to 70 Ry in bulk calculations. In order to have equivalent **k**-point sampling of the Brillouin zone (BZ) for the different lattices that we took into account in our comparative study of the energetics, all the bulk polytypes were simulated in the same hexagonal supercell, having a C_{3v} symmetry and containing 12 SiC bilayers. We tested the accuracy of the total energy bulk calculations with respect to the number of **k** points of the Monkhorst-Pack (MP) grid,[12] and we found that the results converged with a $4\times4\times1$ grid, corresponding to a set of six **k** points in the irreducible wedge of the BZ.

The surface calculations were performed in the repeated supercell approach, using the equilibrium lattice parameters calculated for the respective substrate bulk phases. We used supercells containing seven SiC bilayers, and a vacuum region of thickness 10 Å was included to avoid interactions between periodic replicas. Previous calculations[6] showed that for the SiC(0001) reconstructed surface that we are simulating, the atomic displacements vanish beyond the second bilayer inwards from the topmost plane: therefore, the seven bilayers of our supercell ensure isolation between the two inequivalent surfaces across the slab. For the surface BZ sums, we included the **k** points of a $4\times4\times1$ MP grid.

Both bulk and surface simulations were carried out allowing all the atoms in the supercell to relax. Convergence in the geometry optimization was considered achieved when the forces were smaller than 0.05 eV/Å. The resulting uncertainty in the atomic positions is 0.002 Å. The uncertainty in the total energy difference is (1 meV)/(SiC pair) for the bulk structures. For the surface structures, it is estimated to be less than (10 meV)/(SiC pair), including the uncertainty for assigning a given polytype to the outermost surface bilayer, which indeed has an undefined stacking sequence.

III. BULK CALCULATIONS: SELECTION OF THE MOST ACCURATE XC FUNCTIONAL

Despite the many *ab initio* investigations that have been carried out on the energetics of several metastable bulk phases of SiC, we are aware of no systematic analysis of the effect of the different possible xc functionals. Therefore, as a preliminary step to select the best technical ingredients for studying the surfaces, we evaluated the performance of the LDA, BLYP, and PW91 xc functionals for the calculation of the structural parameters and of the polytype energetics in bulk SiC. We have considered $3C$-, $6H$-, $4H$-, and $2H$-SiC, thus covering a wide range of hexagonality (0% for $3C$, 33% for $6H$, 50% for $4H$, 100% for $2H$).

In Table I, our results are listed in comparison with available LDA and experimental data.[1,2,13–18] The characteristic geometrical parameters of the pH structures are the hexagonal lattice constant a, the lattice constant c perpendicular to the basal plane, and the length $u(j)$ of the Si(j)-C(j) bonds parallel to the c axis $[j=1,\ldots,p/2]$ (see Fig. 1). The results of our calculations are in good agreement with the existing experimental and theoretical data as far as the trends of the lattice constants with the percentage of hexagonality is concerned: for increasing hexagonality, a decreases and the ratio c/pa increases. The bandgap is also an increasing function of the hexagonality percentage. We find that these trends are independent of the exchange-correlation functional. Of the two GGA functionals, the BLYP parametrization overcorrects the LDA approximation, leading to an overestimate of the experimental lattice parameters and to an underestimate of the bulk modulus. Most important, BLYP fails in the description of the relative stability of the polytypes: the zinc blende structure appears to be more stable than the $4H$ phase in BLYP calculations, in disagreement with the general

TABLE I. Calculated ground state properties for the $3C$- and pH-SiC ($p=6,4,2$) bulk polytypes. The values calculated in this work with the LDA, PW91, and BLYP xc functionals, are compared with other DFT-LDA data from the existing literature, and with experimental data. In the last column, the energy per SiC pair is relative to the $4H$ polytype.

	Method	a (Å)	c/pa	$u(j)$ (Å) [$j=1,\ldots,p/2$]	B (Mbar)	E_{gap} (eV)	ΔE_{SiC} (meV)
3C	LDA	3.039	0.8165 [a]		2.31	1.35	+3.2
$p=3$	PW91	3.047	0.8165 [a]		2.23	1.64	+1.0
	BLYP	3.113	0.8165 [a]		1.20	1.78	−1.5
	Exp.	3.083[2]	0.8165 [a]		2.24[13]	2.39[2]	
	LDA [b]	3.063[1]	0.8165 [a]		2.22[14]	1.27[15]	+3.8[14]
6H	PW91	3.044	0.8187	1.873, 1.870, 1.866	2.24	2.23	0
$p=6$	Exp.	3.081[17]	0.8178[17]		2.23[16]	3.02[2]	
	LDA [b]	3.062[1]	0.8172[1]	1.865, 1.860, 1.860[14]	2.18[14]	1.96[15]	+0.8[14]
4H	LDA	3.035	0.8196	1.867, 1.864	2.30	2.23	0
$p=4$	PW91	3.043	0.8198	1.874, 1.870	2.23	2.43	0
	BLYP	3.108	0.8193	1.915, 1.908	1.99	2.57	0
	Exp.	3.081[17]	0.8184[17]		2.23[16]	3.27[2]	
	LDA [b]	3.061[1]	0.8179[1]	1.866, 1.862[14]	2.17[14]	2.18[15]	0
2H	LDA	3.033	0.8217	1.871	2.30	2.29	+6.5
$p=2$	PW91	3.041	0.8219	1.875	2.22	2.54	+7.9
	BLYP	3.105	0.8223	1.917	1.98	2.83	+7.7
	Exp.	3.076[18]	0.8205[18]		2.23[16]	3.33[2]	
	LDA [b]	3.057[1]	0.8201[1]	1.866[14]	2.16[14]	2.10[15]	+5.6[14]

[a]Ideal ratio c/pa= $\sqrt{2/3}$.

[b]DFT-LDA calculated values from the existing literature.

consensus.[14,19] Instead, the PW91 parametrization reproduces the same LDA energetic sorting of the polytypes, and provides an accurate description of the lattice properties, with an average improvement over LDA of 0.3% for the lattice constant a, and of 20% for the bandgap.

These tests allow us to draw the following conclusions: (i) the use of both BLYP and PW91 xc functionals improves the agreement of the calculated bandgap with the experimental data, for all the polytypes taken into account and (ii) the PW91 parametrization maintains the same LDA trends for the lattice constant and for the polytype energetics, whereas the BLYP parametrization fails. The above considerations suggest to select the PW91 functional for the best description of bulk SiC (the same was found for other wide-bandgap semiconductors[20]). Although the effect of gradient corrections is notable only for the electronic properties, and negligible for the structural properties of the bulk crystals, it may become more important in surface systems, where inhomogeneities appear due to the lateral reconstruction. For this reason, we chose the PW91 functional for the surface calculations.

IV. SURFACE CALCULATIONS: GROWTH ISSUES

In agreement with other electronic structure calculations,[14,19] our results for SiC bulk show that the cubic phase has a higher energy than the $4H$ and $6H$ phases at 0 K. Theoretical investigations based on the calculation of the relative free energy show that the cubic phase is unstable also at $T\neq 0$.[1,21] Nevertheless, the systematic appearance of the $3C$ polytype is detected in epitaxially grown films. Furthermore, a stacking transformation from $4H$-SiC to $3C$-SiC was recently detected during the growth of SiC(0001) films on a Si-terminated $4H$-SiC(0001) substrate, resulting in the formation of a $\sqrt{3}\times\sqrt{3}$-reconstructed surface.[4]

Motivated by these results, we focused our attention on the comparative study of the $\sqrt{3}\times\sqrt{3}$ reconstructed surface in $3C$-SiC(111), $4H$-SiC(0001), and $6H$-SiC(0001). There is presently wide agreement about the high stability of this reconstruction, obtained with 1/3 monolayer (ML) of excess Si adatoms at $T4$ sites.[4,6,22,23] Therefore, it is likely to play an important role in the determination of the stable surface growth front in an ordered 2D deposition.[4] At the $\sqrt{3}\times\sqrt{3}$ SiC(0001) reconstruction, each Si adatom is coordinated to three surface Si atoms, and is located above a tetrahedral site of the underlying lattice, occupied by a C atom in the subsurface layer[24] (see Fig. 2). We simulated the real systems using supercells with a 2D $\sqrt{3}\times\sqrt{3}$ periodicity. Our calculations simulate a hydrogen-free environment, at the surface of interest, which is close to the experimental conditions.[4] The dangling bonds of the C atoms at the $(000\bar{1})$ surface were saturated by hydrogen atoms.

The models of the different optimized surfaces are shown in Fig. 3. Below the horizontal dashed line, there are six bulk bilayers of the $3C$-, $4H$-, and $6H$-SiC polytypes. $4H$-SiC has an $ABCB$ stacking sequence and can be terminated at the surface in two nonequivalent ways: either $\cdots BCBAB$

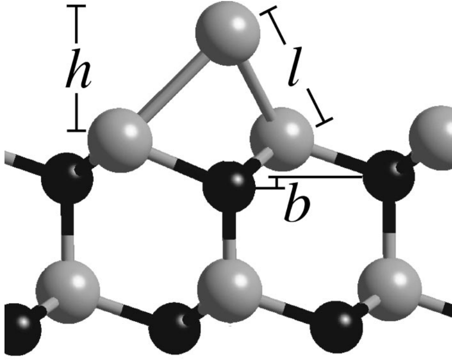

FIG. 2. Side view of the $\sqrt{3}\times\sqrt{3}$ SiC(0001) surface reconstruction. The Si adatom in each unit reconstructed cell saturates the dangling bonds of three Si atoms of the outermost surface layer. The structural parameters reported in Table III are identified.

or $\cdots ABCBA$, labeled $4H_1$ and $4H_2$, respectively. The characteristic unit of $6H$ SiC is stacked, instead, as an $ABCACB$ sequence, which can be interrupted in three nonequivalent ways, among which the $\cdots CACBA$ (labeled 6H $_3$ in Fig. 3) is the only one nonequivalent to any of the $4H_1$ and $4H_2$ options. Above the dashed line in Fig. 3, the outermost surface bilayer can be piled up either preserving (superscript z in the labels) or inverting (superscript w in the labels) the orientation of the immediately underlying bilayer, thus reproducing one step of the $3C$ or $2H$ stacking sequence, respectively. We have eight different systems: $3C^z$ and $3C^w$, $4H_1^z$, and $4H_1^w$, $4H_2^z$, and $4H_2^w$, $6H_3^z$, and $6H_3^w$. Each surface is characterized by the reconstruction (which is the same for all of them), by the relative stacking orientation of the two outermost bilayers (w or z), and by the subsurface stacking sequence ($3C$,$4H_1$,$4H_2$,$6H_3$).

The total energy calculations were performed using the PW91 parametrization of GGA, the choice of which was

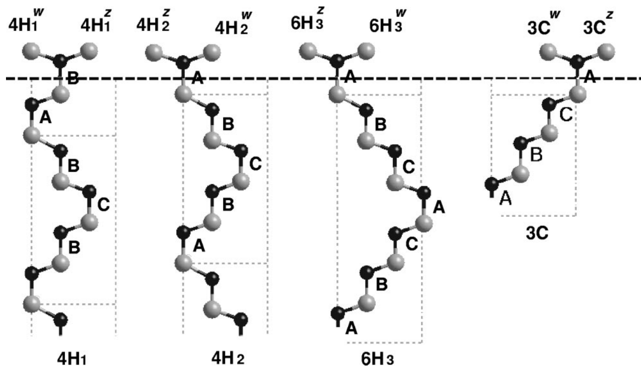

FIG. 3. Side view projection of the eight surface structures that we have studied for $3C$-SiC(111) and pH-SiC(0001), with $p=4$ and $p=6$. The horizontal direction is $[11\bar{2}0]$, the vertical direction is [0001] (equivalent to the [111] for the cubic crystals). Below the dashed line, six bilayers of pH-SiC included in the supercell are shown. The inequivalent ways to truncate the stacking sequence of $4H$ and $6H$ SiC are indicated as $4H_1$ and $4H_2$, $6H_3$. The w and z opposite stacking orientations of the outermost bilayer are shown in each of the four panels.

already motivated in Sec. III. If we conceive the growth of SiC as a layer-by-layer process, with each uniform 2D new bilayer deposited on the surface having the freedom to orient itself into the energetically favorable stacking with respect to the preceding bilayer, and then being buried in that arrangement by the following bilayers, we may take into account the growth of nonequilibrium phases. According to this model, the key quantity to be evaluated is the energy required to form the surface: the new bilayer will be piled up with the orientation that requires the lowest formation energy. The relative surface formation energy of structures having different bulk phases can be evaluated by subtracting the bulk contribution to the total energy of the system: in this way, one obtains a quantity that does not depend on the substrate and therefore is suitable to describe the surface energetics. The relative formation energy $\Delta E_{\rm form}$ of a given $\sqrt{3}\times\sqrt{3}$ surface, with respect to an arbitrary reference structure, may be calculated as

$$\Delta E_{\rm form}=\Delta E_{\rm tot}-N_{\rm SiC}\Delta\mu_{\rm SiC}^{\rm bulk},$$

where $E_{\rm tot}$ is the total energy of the slab obtained by the *ab initio* structural optimization, $N_{\rm SiC}$ is the number of Si-C pairs in the supercell, $\Delta\mu_{\rm SiC}^{\rm bulk}$ is the energy difference per Si-C pair between the substrate bulk phases.

In Table II, the relative formation energies of the different structures included in our study are reported. The reference structure is the $4H_2^z$ configuration. Our results suggest different considerations. First, from a comparison of the energies of the two possible orientations z and w of the outermost surface bilayer, for each of the $4H_1$, $4H_2$, $6H_3$, and $3C$ structures, we can state that the formation energy is lower for the z-like surfaces, for which the topmost bilayer is attached to the underlying bilayer preserving the stacking orientation. This outcome is independent of the substrate polytype. Second, the energy difference between a z-like and a w-like surface stacking is about 30–40 meV per 2D 1×1 cell containing one Si-C pair (28 meV for $3C$, 38 meV for $4H_2$, 41 meV for $4H_1$, and 29 meV for $6H_3$). Such energy differences are one order of magnitude larger than those between the cubic and hexagonal bulk polytypes (few units of meV per Si-C pair). Thus, our results show that on the basis of the energetics, the polytype selectivity is enhanced in the vicinity of a surface. Energy differences of tens of meV per Si-C pair are significant at the growth temperatures, and lead to an energy cost for the inversion stacking of a full surface layer of several eV. This picture may suggest that the polytype selection, during epitaxial growth, is driven by the surface: a growth mechanism based on copying the stacking of the surface bilayer at each deposition step is favored with respect to a stacking inversion. This trend favors the growth of the $3C$ polytytpe, and it may justify the abundance of this phase.[4] Third, the surface formation energy is affected by the relative orientation not only of the two topmost bilayers, but also of deeper layers: analyzing the formation energies of the $4H$-SiC(0001) surfaces listed in Table II, one may see that the lower is the formation energy, the higher is the number of bilayers identically oriented in the proximity of the surface. Indeed, sorting the z-like surfaces by increasing formation

TABLE II. Surface formation energy, relative to the structure $4H_2^z$, calculated according to the equation explained in the text. The surfaces are labeled according to Fig. 3. The total energies were calculated with the PW91 xc functional. The values are normalized to the area of the 1×1 cell, to enhance comparison to the values in the last column of Table I.

Surface	$3C^z$	$3C^w$	$4H_1^z$	$4H_1^w$	$4H_2^z$	$4H_2^w$	$6H_3^z$	$6H_3^w$
ΔE_{form} [meV/(1×1)]	1	29	15	56	0	38	3	32

energy, we see that the energy can be lowered by piling up more than two uniformly oriented bilayers. In fact, the $4H_2^z$, $6H_3^z$, and $3C^z$ structures (having, respectively, 3, 4, and indefinite $3C$-like layers on top) have the lowest energy, degenerate within the precision of these calculations ($\sim$10 meV). Instead, the $4H_1^z$ structure (having only 2 $3C$-like bilayers on top) is energetically unfavorable.

Another interesting observation that we wish to underline is that, whereas for the structures $3C$ and $4H_1$ the energetically favored surface stacking orientation ($3C^z$ and $4H_1^z$, respectively) coincide with the natural continuations of the bulk stacking sequences, in the case of the $4H_2$ and $6H_3$ structures the favorable z choice breaks down the characteristic bulk unit period. This evidence suggests that the energy gain for the deposition of cubic SiC is bigger than the energy cost connected with the formation of a stacking fault defect (an irregularity in an otherwise perfect stacking sequence) at the surfaces of the $4H$ and $6H$ polytypes.

Finally, we point out that our results are in very good agreement with the experimental findings of Starke and co-workers,[4] who detected the presence of a modified stacking sequence on a $4H$-SiC film sample, by means of LEED and scanning tunneling microscopy. In addition to $4H_1$ and $4H_2$ domains, typical of the $4H$ polytype, they found a third kind of domain, consisting of three identically oriented bilayers at the surface. This stacking sequence, whose abundance depended on the growth conditions and sample preparation, is incompatible with the $4H$ substrate and resembles the $3C$ polytype unit cell. Such a domain revealed during MBE growth is what we have called $4H_2^z$. One can imagine two different mechanisms of formation of this new surface stacking: it could develop from the rotation of the topmost bilayer of $4H_1$ or it could be originated when a new identically oriented bilayer is attached on top of the $4H_2$ substrate. Our results are in agreement with the latter interpretation, which was suggested on the basis of the observation[4] that the appearance of the $4H_2^z$ termination is accompanied by a decrease in the extension of the $4H_2$ domain. Because three identically oriented bilayers are typical not only of the purely cubic phase, but also of the $6H$ polytype, for completeness we also took into account the formation of $6H$-SiC(0001) surfaces. From the results in Table II, we conclude that the natural stacking sequence of $6H$-SiC, i.e., $6H_3^w$, is less favorable than the continuation of the cubic sequence ($6H_3^z$). Thus, we can definitely state that during a layer-by-layer deposition surface effects favor the formation of cubic SiC mediated by the presence of the $\sqrt{3}\times\sqrt{3}$ reconstructed surface. The domains with three equally oriented layers observed by Starke and co-workers are not the template for a $4H$-to-$6H$ transition, but for a $4H$-to-$3C$ transition. Additionally, our results suggest that the transition to the cubic phase is also likely in homoepitaxy on $6H$-SiC(0001).

We wish to point out that our findings about the high stability of the cubic stacking at the surface are in disagreement with the conclusions of Rutter and Heine,[25] who sustained that an inversion stacking that would lead to the formation of the $3C^w$ structure is favored at the $3C$-SiC(111) surface. This difference is due to both the different surface structure in the two investigations (they did not consider reconstructed surfaces), and to the use of different relaxation methods.

In Fig. 2, the optimized geometry of the $\sqrt{3}\times\sqrt{3}$ reconstruction is reported. We found that the structural parameters, explicitly labeled in the figure, are independent of the substrate polytype: h is the vertical spacing between the Si adatom and the outermost Si (0001) plane, l is the Si-Si adatom-surface bond length, b is the inward displacement with respect to the ideal lattice of the C atom lying below the Si adatom. The geometry induced by the presence of the adatom is dominated by the local bonding rearrangement in the reconstruction, but the underlying stacking sequence is irrelevant. The parameters of the reconstruction are also independent of the z or w outermost stacking relation, consistently with the observation that an irregularity in the stacking sequence does not destroy the tetrahedral coordination. Our calculated structural parameters are in good agreement with the experimental data[4] (see Table III for a direct comparison). In the relaxation process involved with the reconstruction, the substrate atoms do not move and preserve the bulk-like geometry: only the topmost Si layer and the subsurface C layer undergo structural changes.

For all the surfaces that we selected, we calculated the bandstructure along the $\bar{M}\bar{\Gamma}$ and $\bar{\Gamma}\bar{K}$ symmetry directions of the BZ of the 2D $\sqrt{3}\times\sqrt{3}$ unit cell. No effect of the stacking sequence inside the supercell can be observed in the gap

TABLE III. Structural parameters of the $\sqrt{3}\times\sqrt{3}$-SiC(0001) surface reconstruction, defined in Fig. 2. The results are averaged over the values obtained for the eight studied surfaces (Fig. 3), the largest deviation being 0.02 Å. The DFT-PW91 values obtained in this work are compared to experimental LEED data.

	DFT-PW91 (this work)	LEED (Ref. 4)
h (Å)	1.74	1.77
b (Å)	0.26	0.34
l (Å)	2.42	2.46

region. Instead, the main feature is the appearance of a partially occupied surface band due to the adatom dangling bond, as obtained from previous *ab initio* computations.[26] We find that its energetic location in the middle of the bulk bandgap and its dispersion are independent of the microscopic details of the atomic arrangement for the different surfaces considered in our work. Despite this partially occupied band is obtained as a consequence of the mean-field treatment of correlation effects in DFT-LDA and DFT-GGA, and is known to undergo a Mott-Hubbard splitting,[26,27] the present comparative analysis of its dispersion and of its position relative to the top of the bulk valence band is a reliable outcome of the DFT calculations. Furthermore, the Mott-Hubbard splitting[26,27] does not push the main surface band into the bulk continuum: therefore, even under the correct treatment of correlations, it remains responsible for the surface electronic properties. On the basis of the above considerations, we conclude that the adatom-localized surface band does not interfere with stacking transformations and therefore does not hinder the formation of the surface stacking faults that is necessary for the hexagonal-to-cubic phase transition

V. CONCLUSIONS

We have considered the $3C$ and pH ($p=4,6$) $\sqrt{3}\times\sqrt{3}$-reconstructed SiC(0001) surfaces, taking into account the two opposite stacking sequences of the topmost surface bilayer with respect to the subsurface bilayer. From the differences in formation energy we have detected a preference of the surface for preserving the underlying stacking orientation. This behavior favors the layer-by-layer growth of cubic SiC, independently of the substrate polytype, supporting recent experimental findings of a stacking transformation during homoepitaxy of SiC on the $4H$-SiC(0001) surface. The calculated energy cost for a stacking inversion at the surface is of about 30–40 meV per atom, an amount that is one order of magnitude larger than the energy difference between bulk polytypes, and is sufficient to stabilize the z-like structures with respect to the w-like ones. The geometry and the electronic structure of the surface are not affected by the surface stacking: the reconstruction parameters and the surface bandstructure remain essentially the same changing from a z-like to a w-like termination.

We analyzed the accuracy of the gradient corrections to describe bulk SiC in various metastable phases. We found that the PW91 functional provides an accurate description of the geometric and electronic properties of bulk SiC and of SiC(0001) surfaces. Our results indicate that the PW91 GGA corrections improve the description of SiC with respect to the LDA. Their use does not appear to be mandatory for a reliable description of the bulk, but ensures a higher degree of confidence for the study of surfaces.[28,29]

ACKNOWLEDGMENTS

This work was funded by INFM through the Project for Advanced Research PRA-1MESS and through the Initiative for Parallel Computation. The computing center CINECA is gratefully acknowledged for the use of computing facilities.

[1] F. Bechstedt, P. Käckell, A. Zywietz, K. Karch, B. Adolph, K. Tenelsen, and J. Furthmüller, Phys. Status Solidi B **202**, 35 (1997).

[2] Landolt-Börnstein, *Numerical Data and Functional Relationship in Science and Technology*, new Series, Vol. 17 (Springer-Verlag, Berlin, 1982).

[3] F. Bechstedt and P. Käckell, Phys. Rev. Lett. **75**, 2180 (1995); P. Käckell, J. Furthmüller, and F. Bechstedt, Phys. Rev. B **60**, 13 261 (1999).

[4] U. Starke, J. Schardt, J. Bernhardt, M. Franke, and K. Heinz, Phys. Rev. Lett. **82**, 2107 (1999).

[5] M. Bockstedte, A. Kley, J. Neugebauer, and M. Scheffler, Comput. Phys. Commun. **107**, 187 (1997).

[6] J.E. Northrup and J. Neugebauer, Phys. Rev. B **52**, R17 001 (1995).

[7] A.D. Becke, Phys. Rev. A **38**, 3098 (1988); C. Lee, W. Yang, and R.G. Parr, Phys. Rev. B **37**, 785 (1988).

[8] J.P. Perdew, J.A. Chevary, S.H. Vosko, K.A. Jackson, M.R. Pederson, D.J. Singh, and C. Fiolhais, Phys. Rev. B **46**, 6671 (1992).

[9] N. Troullier and J.L. Martins, Phys. Rev. B **43**, 1993 (1991).

[10] Giovanni Borghi, M.D. thesis, University of Modena, Italy, 2000.

[11] R. Di Felice, C.M. Bertoni, and A. Catellani, Appl. Phys. Lett. **74**, 2137 (1999).

[12] H.J. Monkhorst and J.D. Pack, Phys. Rev. B **13**, 5188 (1976). For the cubic polytype, the lattice constant and total energy converge exactly with a $4\times4\times4$ sampling of the fcc BZ. For the $4H$ hexagonal polytype, full convergence is achieved with a $4\times4\times2$ sampling of the $4H$ BZ. Our choice in this work is beyond these convergence limits.

[13] A. Taylor and R.M. Jones, in *Proceedings of the Conference on Silicon Carbide*, Boston, 1959, edited by J. R. O'Connor and J. Smiltens (Pergamon Press, New York, 1960), p. 147.

[14] P. Käckell, B. Wenzien, and F. Bechstedt, Phys. Rev. B **50**, 17 037 (1994).

[15] P. Käckell, B. Wenzien, and F. Bechstedt, Phys. Rev. B **50**, 10 761 (1994).

[16] D.H. Yean and J.R. Ritter, J. Phys. Chem. Solids **32**, 653 (1971).

[17] A. Bauer, S. Kräusslich, L. Dressler, P. Kuschnerus, S. Wolf, K. Goetz, R. Käckell, S. Furthmüller, and F. Bechstedt, Phys. Rev. B **57**, 2647 (1998).

[18] R.F. Adamsky and K.M. Merz, Z. Kristallogr. **111**, 350 (1959).

[19] S. Limpijumnong and W.R.L. Lambrecht, Phys. Rev. B **57**, 12 017 (1998).

[20] A. Zoroddu, F. Bernardini, P. Ruggerone, and V. Fiorentini, Phys. Rev. B **64**, 045208 (2001).

[21] C. Cheng, V. Heine, and I.L. Jones, J. Phys.: Condens. Matter **2**, 5097 (1990).

[22] A. Coati, M. Sauvage-Simkin, Y. Garreau, R. Pinchaux, T. Argunova, and K. Aïd, Phys. Rev. B **59**, 12 224 (1999).

[23] M. Sabisch, P. Krüger, and J. Pollmann, Phys. Rev. B **55**, 10 561 (1997).

[24] To test the validity of our description of the SiC surfaces, we calculated the formation energy difference between two reconstructions of the $3C_w$ surface. Our test reveals that the reconstruction $T4$ is favored, with respect to the $H3$ one, by 530 meV; this result is in agreement with a previous determination of 540 meV.[6]

[25] M.J. Rutter and V. Heine, J. Phys.: Condens. Matter **9**, 8213 (1997).
[26] M. Rohlfing and J. Pollmann, Phys. Rev. Lett. **84**, 135 (2000).
[27] J.E. Northrup and J. Neugebauer, Phys. Rev. B **57**, R4230 (1998).
[28] V. Aristov, P. Soukiassian, A. Catellani, R. Di Felice, and G. Galli (unpublished).
[29] A. Catellani, G. Galli, and P.L. Rigolli, Phys. Rev. B **62**, 4794 (2000).